

VHE Spectral Energy Distribution of Crab Nebula Compared with the Prediction of a Synchrotron Self-Compton Emission Model

V. G. Sinitsyna, S. S. Borisov, R. M. Mirzafatikhov, F. I. Musin, S. I. Nikolsky, V. Y. Sinitsyna

**P.N.Lebedev Physical Institute,
Leninsky prospect 53, Moscow, 119991, Russia*

Abstract. Crab Nebula has an extraordinary broad spectrum, attributed to synchrotron radiation of electrons with energies from GeV to PeV. This continuous spectrum appears to terminate near 10^8 eV and photons, produced by relativistic electrons and positrons (10^{15} eV) via Inverse Compton, form a new component of spectrum in GeV–TeV energy range. The SHALON observation results of well-known gamma-source Crab Nebula in comparison with other experiments EGRET, COS-B, CELESTE, CAT, Asgat, Whipple, Themistocle, HEGRA CT2, CANGAROO, Tibet, CASA-MIA as well as Magic and HESS are presented. The spectrum of gamma rays from the Crab Nebula has been measured in the energy range 0.8 TeV to 11 TeV at the SHALON Alatau Observatory by the atmospheric Cerenkov technique. The integral energy spectrum is well described by the single power law $I(> E_\gamma) E_\gamma^{-1.44 \pm 0.07}$. Detailed images of gamma-ray emission from Crab Nebula by SHALON telescope are presented. For the purpose of calculating the Inverse Compton scattered radiation, the complete spectrum of Crab Nebula need to be taken into account to deduce the spectrum of relativistic electrons (Hillas et. all. 1998). Then, the TeV gamma-quantum spectrum generated by photons, produced by relativistic electrons and positrons via Inverse Compton is calculated with the assumption of specific average magnetic field in the region of VHE gamma-ray emission, which is taken from the comparison of TeV and X-ray emission regions. The Inverse Compton emission that relativistic electrons would generate in the parts of Crab Nebula is in good agreement with the TeV gamma-ray spectrum observed by SHALON, if the average magnetic field in the region of VHE gamma-ray emission is 67 nT which is extracted from the comparison of TeV (SHALON data) and X-ray (Chandra data) emission regions.

Keywords: Crab Nebula, TeV gamma-rays, Synchrotron Self-Compton Emission Model

I. INTRODUCTION

The observations on Tien-Shan high-mountain station with SHALON Atmospheric Cherenkov Telescopic System had been carried out since 1992 year [1], [2], [3], [4]. The mirror telescopic system of SHALON consists of a composed mirror with the area of $11.2m^2$. It is

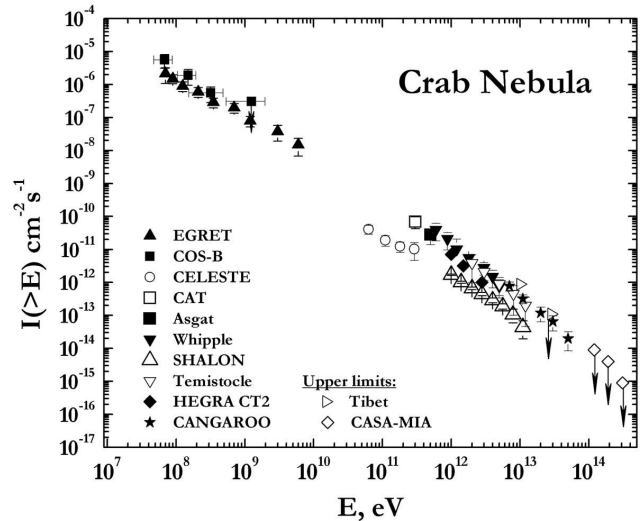


Fig. 1: The Crab Nebula gamma-quantum integral spectrum by SHALON in comparison with other experiments: EGRET, COS-B, CELESTE, CAT, Asgat, Whipple, Themistocle, HEGRA CT2, CANGAROO, Tibet, CASA-MIA [1 – 13]

equipped with a 144-photomultiplier light-receiver that has the field of view $> 8^\circ$ (the largest in the world). It enables one to continuously control the background of cosmic-ray particle emission and the atmosphere transparency, thus increasing the observation efficiency. During the period since 1992 12 metagalactic and galactic sources have been observed. Among them are galactic sources Crab Nebula (supernova remnant), Cygnus X-3 (binary), Tycho's SNR (supernova remnant), Geminga (radioweak pulsar) and 2129+47 (binary) [1], [2], [3], [4], [5], [6], [7]. The results of observation data analysis for the each source are integral spectra of events coming from source - k_{ON} , and background spectra of events, coming simultaneously with source observation - k_{OFF} , temporal analysis of these two kind events and the source images. At Figs. 1, 2, and table I, the observation results of Galaxy gamma-sources are showed.

II. CRAB NEBULA

As in many other bands of electromagnetic spectrum, the Crab Nebula has become the standard candle for TeV

TABLE I: The flux from Crab Nebula

Group	VHE Spectrum ($10^{-11} \text{ photons cm}^{-2} \text{ s}^{-1} \text{ TeV}^{-1}$)	E_{th} (TeV)
Whipple (1991)	$25 \times (E/0.4 \text{ TeV})^{-2.4 \pm 0.3}$	0.4
Whipple (1998)	$(3.2 \pm 0.7) \times (E/\text{TeV})^{-2.49 \pm 0.06_{stat} \pm 0.04_{syst}}$	0.3
SHALON (2005)	$(1.7 \pm 0.12) \times 10^{-1} \times (E/\text{TeV})^{-2.44 \pm 0.07}$	0.8
CANGAROO (1998)	$(2.01 \pm 0.36) \times 10^{-2} \times (E/7 \text{ TeV})^{-2.53 \pm 0.18}$	7.0
CAT (1999)	$(2.7 \pm 0.17 \pm 0.40) \times (E/\text{TeV})^{-2.57 \pm 0.14_{stat} \pm 0.08_{syst}}$	0.25
HEGRA (1999)	$(2.7 \pm 0.2 \pm 0.8) \times (E/\text{TeV})^{-2.60 \pm 0.05_{stat} \pm 0.05_{syst}}$	0.5
Magic (2005)	$(1.5 \pm 0.18) \times 10^{-3} \times (E/\text{GeV})^{-2.58 \pm 0.16}$	0.3
HESS (2005)	$(2.86 \pm 0.06 \pm 0.57) \times (E/\text{TeV})^{-2.67 \pm 0.01_{stat} \pm 0.1_{syst}}$ $(3.76 \pm 0.07) \times (E/\text{TeV})^{-2.39 \pm 0.03_{stat}} \times \exp(E/(14.3 \pm 2.1))$	0.44
Tibet HD (1999)	$(4.61 \pm 0.1) \times 10^{-1} \times (E/3, \text{TeV})^{-2.62 \pm 0.17}$	3.0

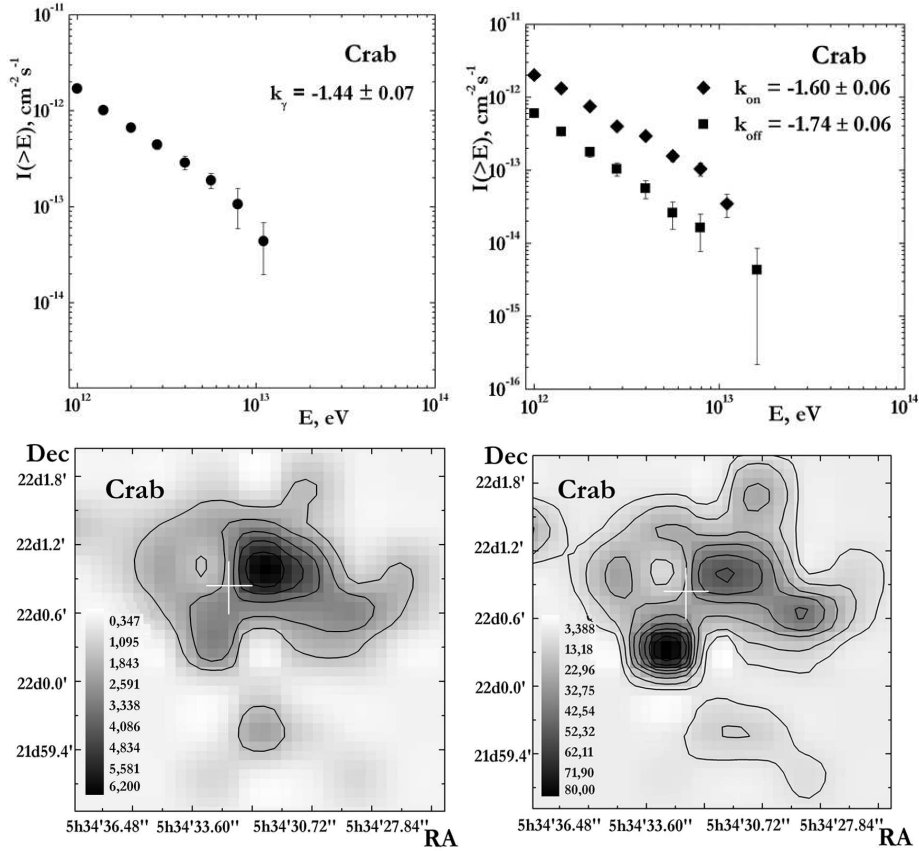


Fig. 2: **Top. left** – The Crab Nebula gamma-quantum integral spectrum with power index of $k_\gamma = -1.44 \pm 0.07$; **right** – The event spectrum from Crab Nebula with background with index of $k_{ON} = -1.60 \pm 0.06$ and spectrum of background events observed simultaneously with Crab Nebula with index $k_{OFF} = -1.74 \pm 0.06$. **Bottom. left** – The image of gamma-ray emission from Crab; **right** – The energy image (TeV units) of Crab by SHALON.

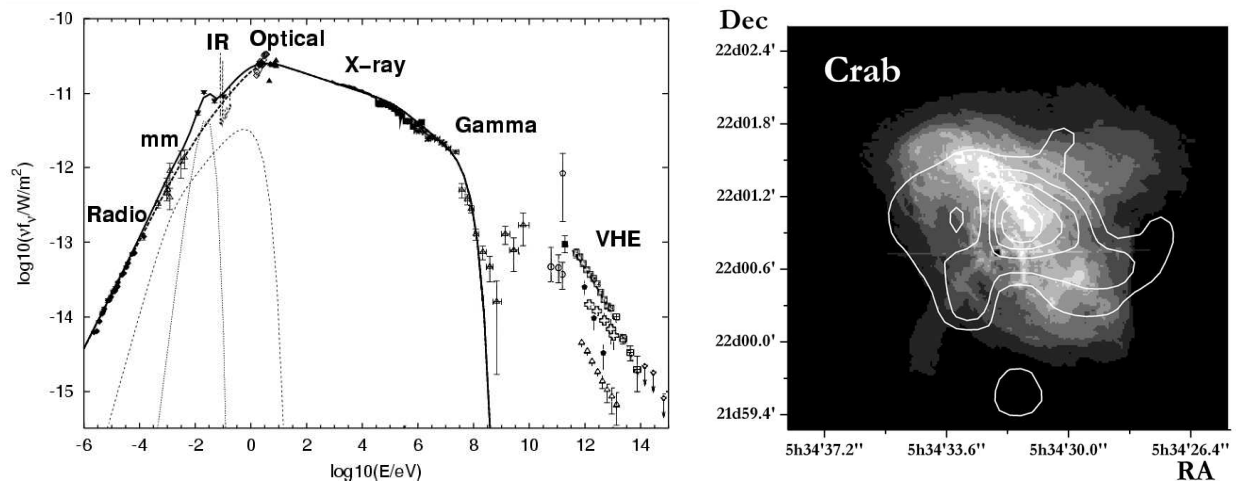


Fig. 3: **left** – The Crab Nebula γ -quantum integral spectrum by SHALON in comparison with other experiments: EGRET, COS-B, CELESTE, CAT, Asgat, Whipple, Themistocle, HEGRA CT2, CANGAROO, Tibet, CASA-MIA [1 – 13]; **right** – A Chandra X-ray image of Crab Nebula. The central part $200'' \times 200''$ of Crab Pulsar Wind Nebula (PWN) in the energy range 0.2-20 keV. The white contour lines show the TeV - structure by SHALON observations.

gamma-ray astronomy. It is available as steady source to test and calibrate the telescope and can be seen from both hemispheres. Since the first detection with ground based telescope the Crab has been observed by the number of independent groups using different methods of registration of gamma-initiated showers. Some of these detections are presented below and shown on fig. 1. The SHALON observation results of well-known gamma-source Crab Nebula are presented at Figure 1 in comparison with other experiments EGRET, COS-B, CELESTE, CAT, Asgat, Whipple, Themistocle, HEGRA CT2, CANGAROO, Tibet, CASA-MIA. The spectrum of gamma rays from the Crab Nebula has been measured in the energy range 0.8 TeV to 11 TeV at the SHALON Alatoo Observatory by the atmospheric Cerenkov technique. The integral energy spectrum is well described by the single power law $I(> E_\gamma) \propto E_\gamma^{-1.44 \pm 0.07}$ (Fig. 2, table I). The spectrum indices for Crab Nebula obtained by Whipple, SHALON, CANGAROO, CAT, HEGRA atmospheric Cerenkov telescopes, Magic, HESS and Tibet are presented in table I and [4 – 16] Also, the results of observation data analysis are the images of Crab. A detailed image of gamma-ray emission from Crab Nebula by SHALON telescope is shown in Fig. 2.

Crab Nebula has an extraordinary broad spectrum, attributed to synchrotron radiation of electrons with energies from GeV to PeV. This continuous spectrum appears to terminate near 10^8 eV and photons, produced by relativistic electrons and positrons ($\sim 10^{15}$ eV) via Inverse Compton, form a new component of spectrum in GeV - TeV energy range.

For the purpose of calculating the Inverse Compton scattered radiation, the complete spectrum of Crab Nebula need to be taken into account to deduce the spectrum

TABLE II: Magnetic Fields and Lifetimes [17]

Region	Field (10^4 Gauss)	Lifetime (years)	Extent of region (light years)
PWN average	5.8	6.7	1.9 (60'' radius)
bright Torus	7.7	4.3	1.7 (radius)
NW Loops	9.1	2.9	0.6
Jet center, region 7	9.1	2.9	1.8 (length of jet)
bright inner ring	10.8	2.6	0.08 (thickness of ring)
knot in bright inner ring	15.3	1.5	0.07 (size of knot)
S Finger, region 5	6.2	5.9	1.3 (length of finger)
SW Finger, region 7	6.2	5.9	1.6 (length of finger)

of relativistic electrons (see ref. [11]). First, assuming magnetic field strength in the region of emission, shown in fig. 2, 3 and a distance of 2 kpc to the nebula, the number spectrum of electrons in the nebula can be deduced. Then the spectrum of emitted Inverse Compton scattered photons can be deduced from the electron spectrum [11].

In order to find relation between TeV and X-ray emission and characteristics which are necessary to calculate a VHE gamma-ray spectrum, the combination of SHALON and Chandra images were analyzed.

Figure 3 presents a Chandra X-ray image of the central part $200'' \times 200''$ of Crab Nebula in the energy range 0.2-20 keV. In this energy band most of the PWN X-rays come from a torus surrounding the pulsar. The white contour lines show the TeV - structure by

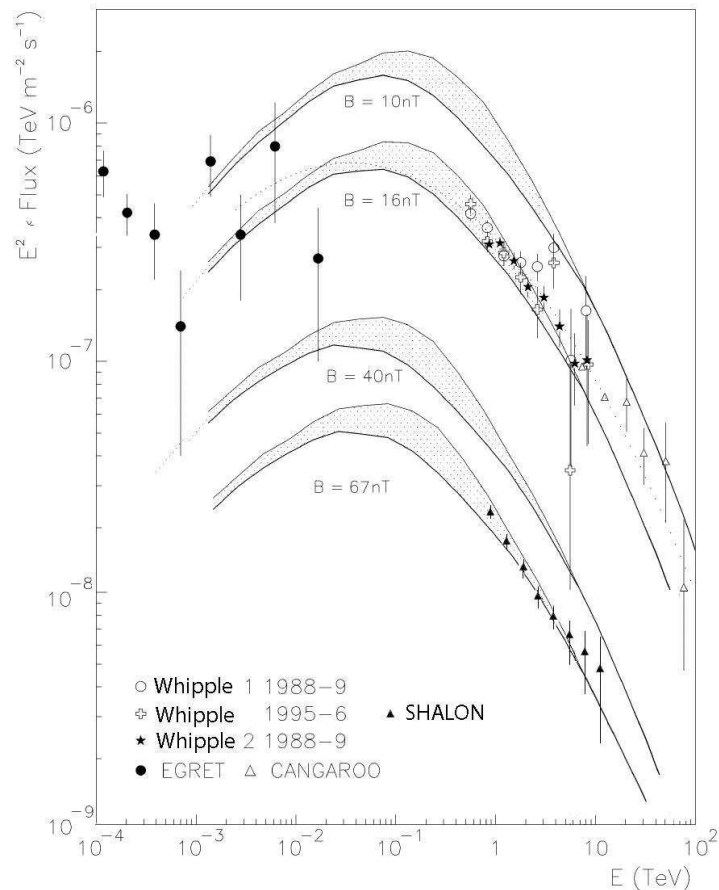


Fig. 4: The Crab Nebula gamma-quantum spectrum by SHALON together with other experiments: Whipple, EGRET, CANGAROO and with the predicted inverse Compton spectrum for the different field strengths [11] and for the 67 nT.

SHALON observations. The most part of TeV energy gamma-quanta come from the region of bright torus (see fig. 3, table II) whereas the contribution of energy gives the region of the southern jet (see fig. 2).

Magnetic fields and lifetimes of representative regions in Chandra image of Crab have been derived [17] and are listed in Table II.

III. CONCLUSION

The TeV gamma-quantum spectrum (see fig. 4) generated by photons, produced by relativistic electrons and positrons via Inverse Compton is calculated with the assumption of specific average magnetic field in the region of VHE gamma-ray emission, which is taken from the comparison of TeV and X-ray emission regions. The Inverse Compton emission that relativistic electrons would generate in the parts of Crab Nebula is in good agreement with the TeV gamma-ray spectrum observed by SHALON, if the average magnetic field in the region of VHE gamma-ray emission is 67 nT which is extracted from the comparison of TeV (SHALON data) and X-ray (Chandra data, fig. 3 and table II) emission regions.

REFERENCES

- [1] V. G. Sinitsyna, AIP Conf. Proc., 515, (1999) pp. 205 and 293.
- [2] V. G. Sinitsyna, S. I. Nikolsky, et al., *Izv. Ross. Akad. Nauk Ser. Fiz.*, 66(11), (2002) pp. 1667 and 1660.
- [3] V. G. Sinitsyna, et al., in Proc. 27th Int. Cosmic Ray Conf., Hamburg, 3, (2001) p. 2665; in Proc. 29th Int. Cosmic Ray Conf., Puna, 4, (2005) p. 231.
- [4] V. G. Sinitsyna et al., *Nucl. Phys. B (Proc. Suppl.)*, 151, (2006), p. 112;
- [5] V. G. Sinitsyna et al., *Nucl. Phys. B (Proc. Suppl.)*, 122, (2003) p. 247;
- [6] S. I. Nikolsky and V. G. Sinitsyna, *Nucl. Phys. B (Proc. Suppl.)*, 122, (2003) p. 409;
- [7] V. G. Sinitsyna et al., *Nucl. Phys. B (Proc. Suppl.)*, 97, (2001) pp. 215, 219.
- [8] T. C. Weekes, AIP Conf. Proc., 515, (1999) p. 3.
- [9] M. Catanese and T. C. Weekes, Preprint Series, no. 4811, (1999).
- [10] J. Prah and C. Prosch (for the HEGRA Collaboration), in Proc. 25th Int. Cosmic Ray Conf., Durban, 3, (1997) p. 217.
- [11] A. M. Hillas, et al., *ApJ*, 503, (1998) p. 744.
- [12] T. Tanimori, et al., *ApJ*, 492, (1998) p. 133.
- [13] F. Piron, et al., in Proc. 28th Int. Cosmic Ray Conf., Tsukuba, (2003) p. 2607.
- [14] F. Aharonian, A. G. Akhperjanian, et al. *Astronomy & Astrophysics N^o. 5351CPM*
- [15] C. Masterson, et al., in Proc. 29th Int. Cosmic Ray Conf., Puna, 4 (2005) p. 143.
- [16] R. M. Wagner, et al., in Proc. 29th Int. Cosmic Ray Conf., Puna, 4 (2005) p. 163.
- [17] F. D. Seward, W. H. Tucker and R. A. Fesen arXiv:astro-ph/0608485